*International Journal of Microwave and Wireless Technologies*

**cambridge.org/mrf**

# Multiband symmetrical slotted antennas for independent frequency tuning and wireless communication

Geriki Polaiah

Electronics and Communication Engineering, Vignan's Foundation for Science Technology and Research, Hyderabad, Telangana, India

**Research Paper**

**Cite this article:** Polaiah G (2026) Multiband symmetrical slotted antennas for independent frequency tuning and wireless communication. *International Journal of Microwave and Wireless Technologies* **18**(5), 793–802. https://doi.org/10.1017/S1759078726103547

Received: 31 December 2025 UTC
Revised: 1 June 2026 UTC
Accepted: 18 June 2026 UTC
First published online: 23 July 2026 UTC

**Keywords:**
compact structure; independent frequency tuning; multiband; quatrefoil shape; slotted antenna

Email: polaiahgeriki@gmail.com

**Abstract**

It is proposed to use a triple-band, quatrefoil-shaped planar slotted monopole antenna that has independent frequency tuning and operates at 1.6, 2.4, and 5.6 GHz for wireless communication systems. To achieve the dual-band resonance, the antenna consists of four comparable circular slots etched on four additional symmetrical circular patches. For the third independent frequency band, the antenna uses an open-ended inverted L-slot on the feed line. The antenna peak gains of 2.8, 3.1, and 3.7 dB are obtained at matching frequencies, according to measured data. The feed-length variation-based dual-band slot antennas operating at UMTS2.1 GHz and Wi-Fi 2.45 GHz frequencies individually for radio frequency energy harvesting have been presented in this work. Besides, these antennas also provide wireless communication with the second band. The measured results of the proposed designs are compared with the corresponding simulation results. The parametric analysis of the simulated reflection coefficient has been performed at the different feed lengths of the two antennas. The gains of antennas are greater than 3.5 dBi and the radiation efficiency of the antenna is more than 71% obtained at the center frequency of all the operating bands.

## Introduction

Compact, low-profile, planar multiband antennas with independent frequency tuning are in greater demand due to the rapid development of advanced mobile communication systems. By utilizing adaptable elements like varactor diodes (for constant tuning of frequencies) or PIN diodes (for distinct switching) within its structure, an autonomous frequency tuning multichannel antenna dynamically modifies each operating frequency band independently, overcoming the limitations of fixed designs. It frequently uses methods such as irregular structures, slotted insertion, or resonator connections (Split Ring Resonators (SRRs), Circular Split Ring Resonators (CSRRs)) to establish different alternate resonant modes for applications requiring adjustable, broadband, or multi-service coverage, as seen in 5G, surveillance, and Internet of Things devices. A simple design of planar antenna with fewer integration losses is immensely required to connect widely used microwave devices like rectifier, diplexer, filter, etc., in various applications. In recent years, dual- and triple-band antennas with independent frequency tuning have been reported in [1–6], but the antenna size is large, and the etching of copper layer on the two sides of the substrate is needed. In [1, 3, 5], passive components of capacitors and inductors are primarily inserted on the antenna radiator for independent controll of dual- and triple-band frequencies, which results in radiation losses. However, a single substrate compact hand-held multiband antenna is extensively desirable for easy integration with other devices. Recently, proximity coupled [7] and rectangular slot-loaded [8], triple-band antennas have been reported for multiband operation, but these designs include two back-to-back substrate layers, and also the antenna size in [8] is large. Strip line-based slotted antenna with similar split ring resonators [9], a dual-band U-shaped slot rectangular patch antenna [10], a quad-band antenna using two substrates [11], and a triple-band patch antenna [12] are presented. Similarly, a unidirectional dual-band stacked patch antenna [13], quad-band antenna with independent frequency tuning [14], slotted monopole antenna [15], and Vivaldi antenna [16] are reported. Similarly, a slot-line based Multiple Input Multiput Output (MIMO) antenna with independent frequency tuning [17], a dual-band reconfigurable flexible antenna [18], an end-fire stepped slot antenna [19], and a thin film based antenna [20] are reported. The structures in [11] and [12] show a complex and soldering with more lumped components for frequency tuning. An appropriate gain,

© The Author(s), 2026. Published by Cambridge University Press in association with The European Microwave Association.

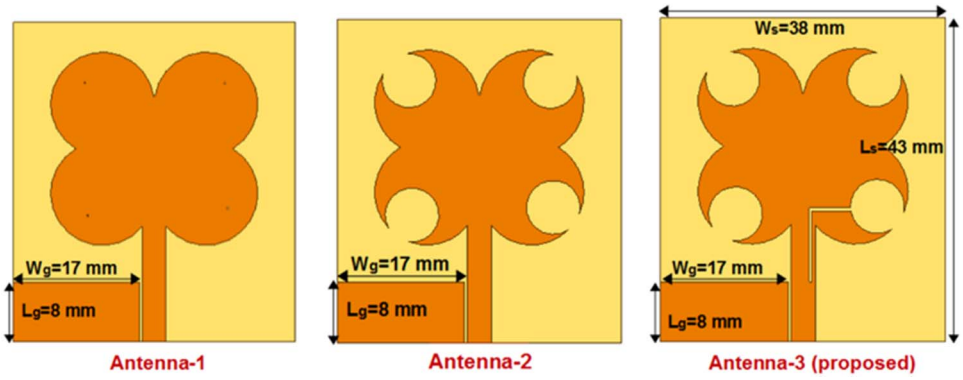



**Figure 1.** Geometrical configurations of the three different monopole antennas.

monopolar radiation pattern, and good radiation efficiency are necessary for a small-sized planar antenna in order to support sophisticated wireless communication such as the Internet of Things, 5G, and distant sensor nodes. In order to receive radio frequency (RF) power from the 1.95 and 2.45 GHz frequency bands, a gain-enhanced dual-band microstrip antenna with a reflector was described in [21]. A paper-based small triple-band antenna that operates in the Long Term Evolution (LTE) bands was described in [22]. The double-band monopole antenna for the 1.8 and 2.1 GHz cellular frequencies was introduced in [23]. A microstrip patch antenna with dual ports and tri-band capability for mobile frequencies of 0.9 GHz, 1.8 GHz, and 2.1 GHz was detailed in [24]. A loop antenna is situated on an artificial magnetic conductor surface as reported in [25]. In [26], a folded dipole antenna with slot loading that operates at 0.915 and 2.45 GHz was demonstrated. For wireless sensor networks, a quad-band dipole antenna operating at three cellular bands and one lower Wi-Fi band was introduced in [27]. Comparably, [28–31] and [32] propose compact antennas with harmonic suppression.

In this work, a compact quatrefoil shape triple-band planar monopole antenna with independent frequency tuning using circular slots and open-ended inverted L-slot is proposed for multiband wireless communication systems. To excite the necessary triple bands, the antenna is made up of a Coplanar Wave Guide (CPW) fed with a single-sided ground plane. There is no copper layer printed on the back of the substrate; the antenna is designed on the front side. The symmetrical structure of the antenna leads to an enhancement in both compactness and radiation performance. This work also presents double-band slotted antennas with adjustable feed length (FL) that operate at the mobile and Wi-Fi bands.

## Triple-band antenna with independent frequency tuning

### *Antenna design details*

Figure 1 shows the geometrical arrangements of the three distinct monopole antennas. The suggested antenna is built on an FR4 substrate material that has the following properties: loss tangent ($\tan\delta$)=0.025, thickness($t$)=1.6 mm, and dielectric constant ($\varepsilon_r$)=4.3. The antenna is made up of four partially overlapping circles with the same radius, or a simple structured quatrefoil shape. These are etched by other symmetrical circular slots and consist of symmetrical circular patches. As seen in antenna-1, the first band of the antenna is produced by combining four circles with identical radii of 7 mm.

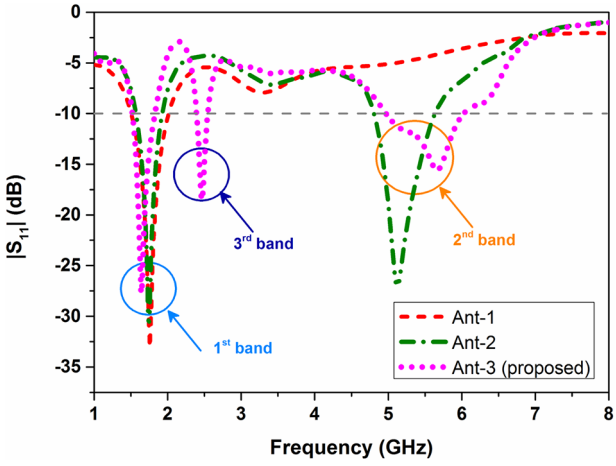



**Figure 2.** Simulation results – antenna three different configurations.

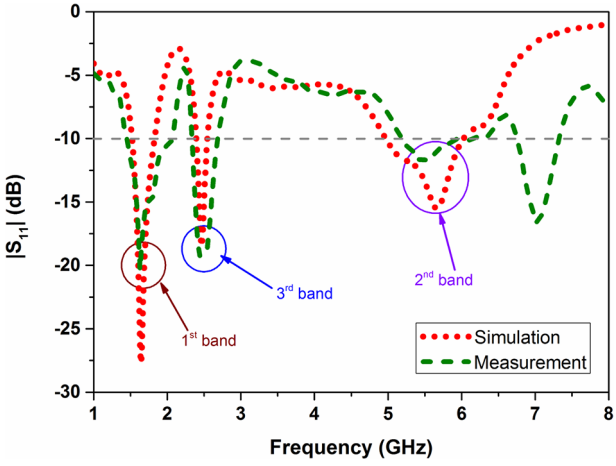



**Figure 3.** Simulation and measured reflection coefficient (antenna-3-proposed).

The antenna is integrated into a 50Ω microstrip feed line to provide the highest input power possible for the excitation of the necessary tri-band frequencies. On the left side of the feed line, a ground plane measuring 8 mm×17 mm (Lg×Wg) with a 0.4 mm gap width is designed. The suggested antenna has geometric dimensions of 47 mm×36 mm (Ls×Ws). All that is needed to create the antenna's second band is a straightforward etching

https://doi.org/10.1017/S1759078726103547 Published online by Cambridge University Press

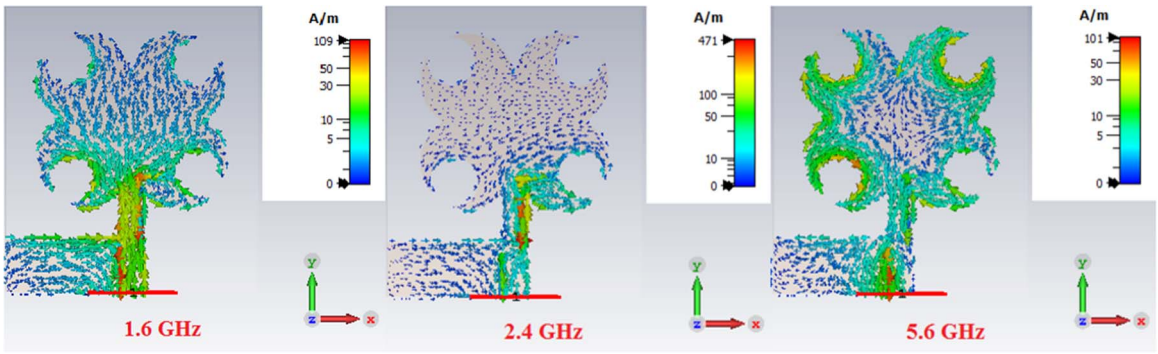



**Figure 4.** Surface current distribution of proposed antenna at three resonant frequencies.

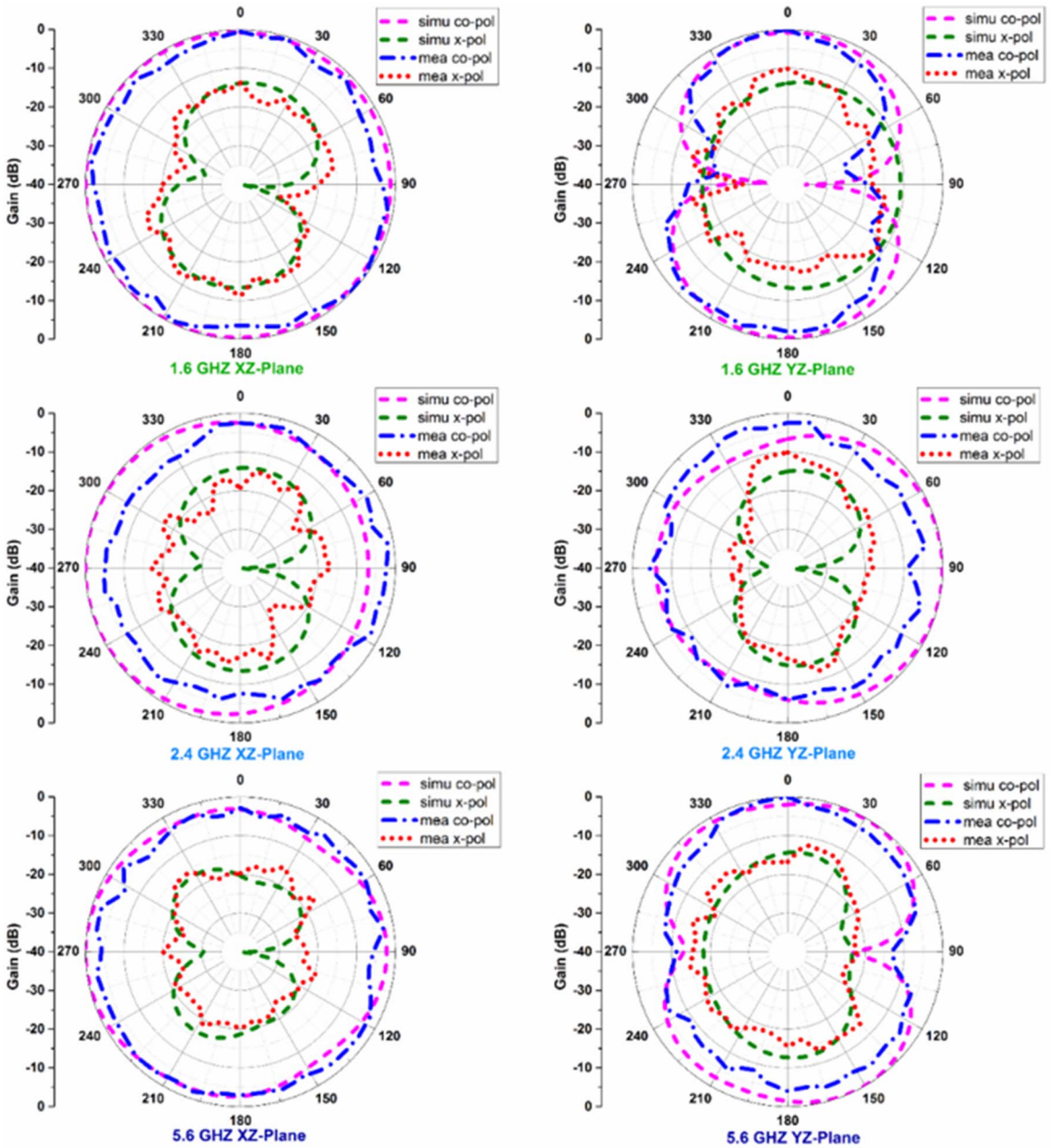



**Figure 5.** Simulation and measured normalized radiation patterns.

https://doi.org/10.1017/S1759078726103547 Published online by Cambridge University Press

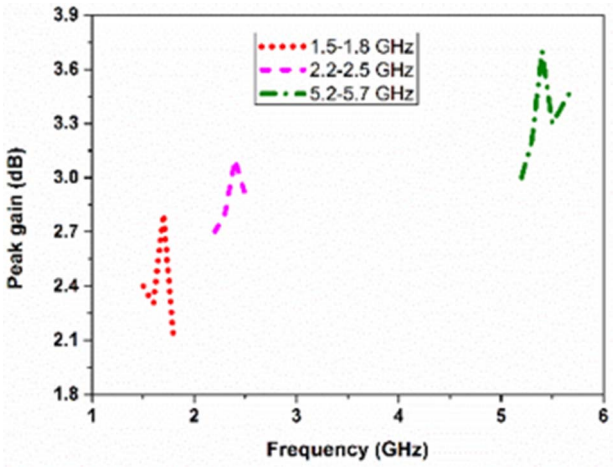



**Figure 6.** Measured gain of the proposed antenna.

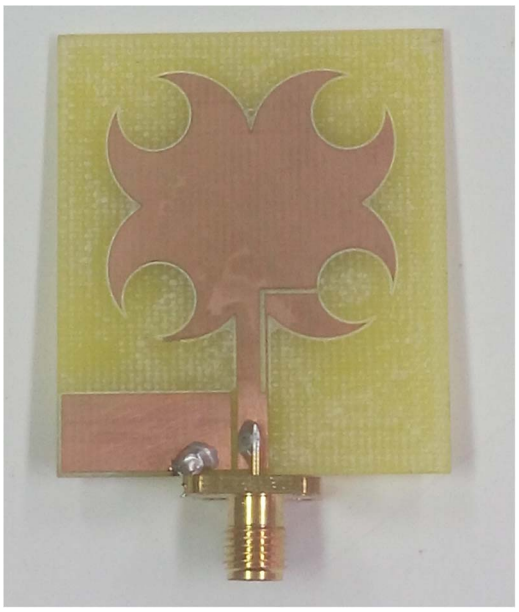


**Figure 7.** Fabrication photograph of the proposed antenna.

process using symmetrical slotted circles with a 3.6 mm radius. The ground plane size and the circular patch dimensions remain unchanged in this instance. Another configuration of this design layout is antenna-2. Finally, for the third frequency band, which is represented by Antenna-3 (proposed) in Figure 1, an inverted open-ended L-slot covering the feed line and circular slot is etched with a width of 0.4 mm. These three functioning frequency bands simply rely on their matching geometrical dimensions and are independently controlled by one another. Because of the efficient coupling of the inverted L-slot and circular slots with the radiator, the proposed antenna has constant frequency bands.

## Results and discussion

Figure 2 shows the reflection coefficient ($|S_{11}|$) simulation results for the three antenna layouts. The antenna-1 arrangement shown in Figure 1 has the fundamental resonance at 1.75 GHz without any higher-order harmonics. Similar to the first band, which is slightly displaced to the lower frequency side, the antenna-2 arrangement resonates with the second band independently at 5.1 GHz because of the etching of slotted circles. Without significantly altering the first and second band frequencies, the third band frequency of 2.4 GHz can be simply attained by etching an open-ended, inverted L-shaped slot on the patch and feed line. The proposed antenna (antenna-3 design) functioning at the distinct triple-band frequencies of 1.6, 2.4, and 5.6 GHz with independent control is finally described by the simulation results. Agilent Technologies vector network analyzer is used to measure $|S_{11}|$ versus frequency for the proposed slotted antenna. Figure 3 shows the simulation and measured results of the proposed antenna's reflection coefficient ($|S_{11}|$).

The measured result for the impedance matching of the second band frequency is slightly pushed upward, but still below 10 dB, while the remaining bands match the results of the simulation. Additionally, the performance of the suggested slotted antenna is examined using the surface current distribution at the triple-band frequencies of 1.6, 2.4, and 5.6 GHz. Figure 4 shows the results of a simulation conducted on the surface current of the suggested antenna at three different operating frequencies. At its lower band frequency of 1.6 GHz, it is seen that the current vector is primarily dispersed on the lower part of the antenna radiator. Similar to this, the group of current vectors is directed on the 2.4 GHz frequency band, which is produced by an open-ended, inverted L-shaped slot. On the borders of the symmetrical circular open slots, which largely resonate with the operating frequency of 5.6 GHz, is where the major current dispersion is found. Additionally, it should be verified by the surface current distribution that the suggested compact planar slotted monopole antenna is tuned independently and operating at the most practical triple-band frequencies.

Figure 5 shows the simulated and measured radiation patterns of the proposed antenna at the two primary planes, the H-plane

**Table 1.** Comparison of the proposed triple-band antenna with recently reported antennas

| Ref. | Antenna type | Dimension (mm$^2$) | Freq (GHz) | Gain (dB) | Efficiency | Substrate | Bandwidth (GHz) | Application |
|---|---|---|---|---|---|---|---|---|
| [11] | Yagi antenna | 194×106 | 1.8–2.2 | 10.5 | 84% | Rogers | 0.4 | Communication |
| [12] | Dual slot | 138×95 | 2.0–2.7 | 10.3 | 74% | Rogers | 0.7 | WLAN |
| [13] | Dual-polarized | 70×70 | 1.8–2.5 | 4.1 | 82% | FR4 | 0.7 | Communication |
| [14] | Microstrip patch | 87×87 | 1.1–2.7 | 8.6 | 87% | Rogers | 1.6 | Communication |
| [15] | Slotted monopole | 50×35 | 2.0–3.1 | 4.0 | 79% | FR4 | 1.1 | WLAN |
| [16] | Vivaldi antenna | 55×40 | 2.3–2.85 | 3.0 | 74% | FR4 | 0.55 | WLAN |
| This work | Triple band | 47×36 | 1.6, 2.4, 5.6 | 3.7 | 83% | FR4 | 0.6, 0.3, 0.5 | Freq Tuning |

https://doi.org/10.1017/S1759078726103547 Published online by Cambridge University Press

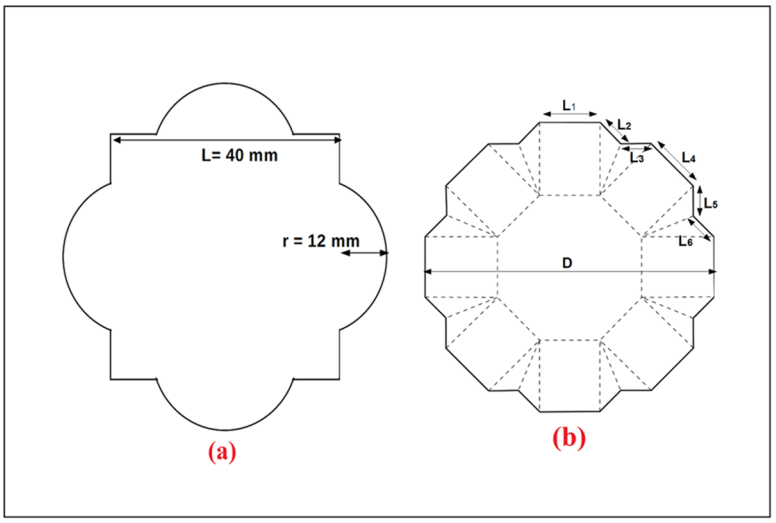



**Figure 8.** The basic geometry of the proposed antennas: (a) antenna-1 and (b) antenna-2. The side lengths of antenna-2 are $L_1 = 10$ mm, $L_2 = 7$ mm, $L_3 = 5$ mm, $L_4 = 7$ mm, $L_5 = 5$ mm, $L_6 = 7$ mm, and diameter $D = 50$ mm.

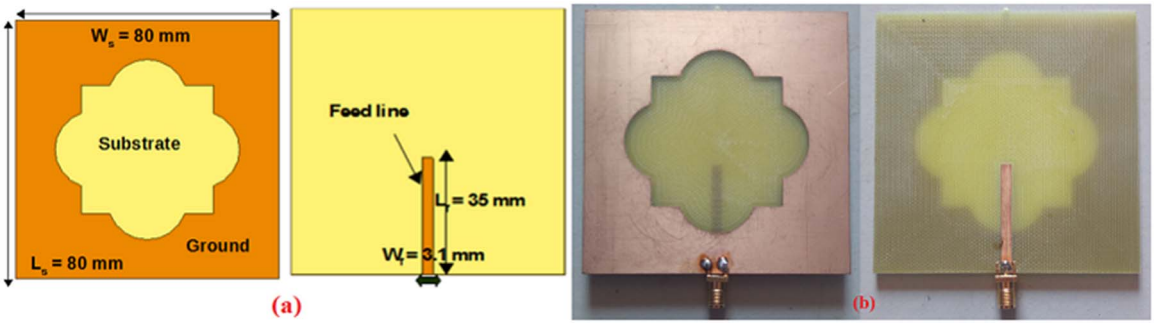



**Figure 9.** Configurations of the proposed antenna-1: (a) schematic and (b) fabrication prototypes.

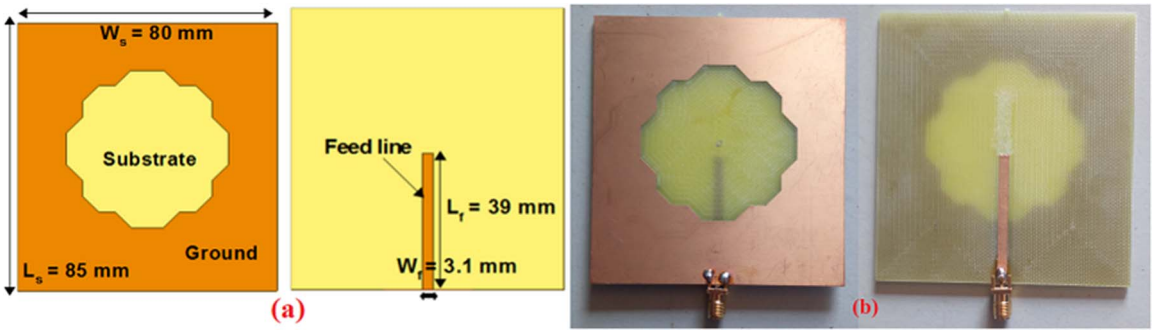



**Figure 10.** Configurations of the proposed antenna-2: (a) schematic and (b) fabrication prototypes.

(YZ-plane, $\phi$=90$^0$) and the E-plane (XZ-plane, $\phi$=0$^0$), at three resonating frequencies. The proposed monopole antenna's radiation patterns, which are appropriate for portable mobile or tablet devices, exhibit bi-directional patterns in the YZ-plane and omni-directional patterns in the XZ-plane. Gain and radiation patterns are measured using a typical double-ridged broadband transmitting horn antenna with a gain variation of 2–20 dB in the 1.0–20 GHz frequency range. Three operating frequencies are covered by the far-field condition because of the selected distance between the transmitting and receiving antennas. In comparison to the co-polarization (co-pol) of three operating frequencies, a cross-polarization (x-pol) of less than 10 dB was achieved in both planes through simulation and measurement. Figure 6 shows the measured peak gains of the proposed slotted antenna at three operating frequencies. At equivalent frequencies of 1.6, 2.4, and 5.6 GHz, respectively, the antenna peak gains of 2.8, 3.1, and 3.7 dB are attained. Table 1 compares the proposed slotted antenna with recently published multiband antennas. Despite having a smaller antenna, [7] uses two substrates to implement it. The peak gain of 3.7 dBi was obtained at 5.6 GHz. It was measured in the anechoic chamber using the E8363C PNA network analyzer. The fabrication photograph of the proposed antenna is shown in Figure 7. The proposed antenna has three advantages over existing multiband antennas: smaller size, increased gain, and single substrate use. The proposed antenna's symmetrical quatrefoil design results in steady radiation patterns. The slots in the shape of a crescent

https://doi.org/10.1017/S1759078726103547 Published online by Cambridge University Press

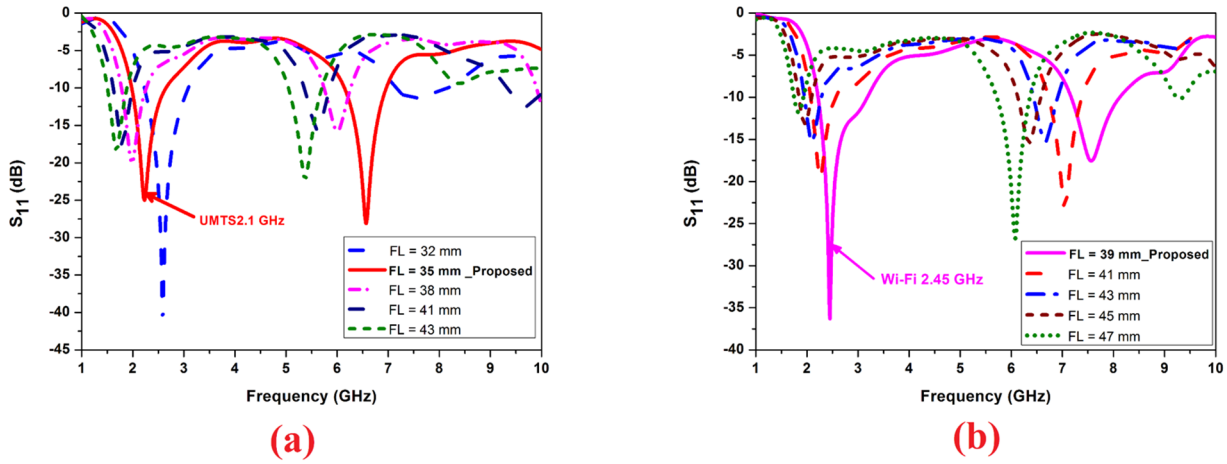



**Figure 11.** Simulated reflection coefficient $S_{11}$ varies with the FL: (a) antenna-1 and (b) antenna-2.

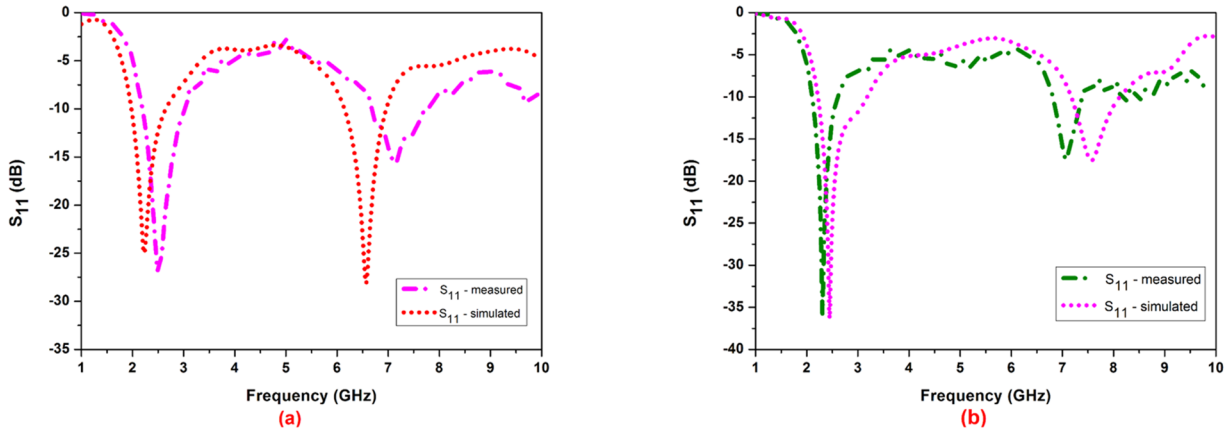



**Figure 12.** Simulated and measured reflection coefficient of proposed antennas: (a) antenna-1 and (b) antenna-2.

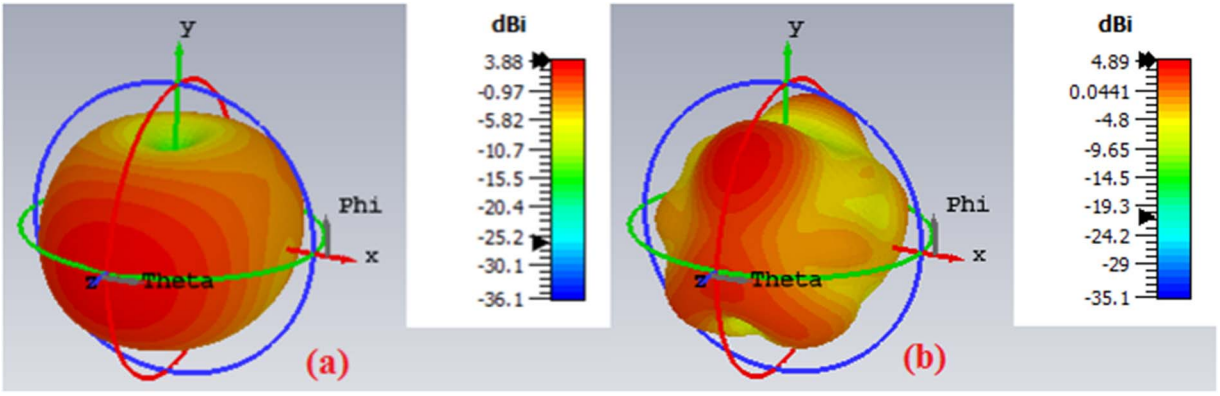



**Figure 13.** Simulated 3D-gain radiation patterns of the proposed antenna-1: (a) 2.16 GHz and (b) 6.57 GHz.

moon are accurately carved at the margins of circles that have comparable diameters. The slotted circles in the shape of a crescent moon produce reliable triple bands with good impedance matching. For every resonant frequency, a realized gain of over 2 dB was attained. Applications involving wireless power transfer and energy harvesting can benefit from the antenna proposed in this paper. For a variety of microwave communication applications, this antenna can be readily combined with other microwave devices such as rectifiers, diplexers, and filters, etc. Wireless communication and RF energy harvesting are further possible applications for the proposed antenna. We have a lot of RF power available from cell towers and Wi-Fi routers everywhere in an environment with short distances. The rooftop of a building is where the cell towers are located in an urban setting. Wirelessly connected low-power electronic devices can be powered by this wasted RF energy if it is used appropriately. RF energy harvesting and wireless

https://doi.org/10.1017/S1759078726103547 Published online by Cambridge University Press

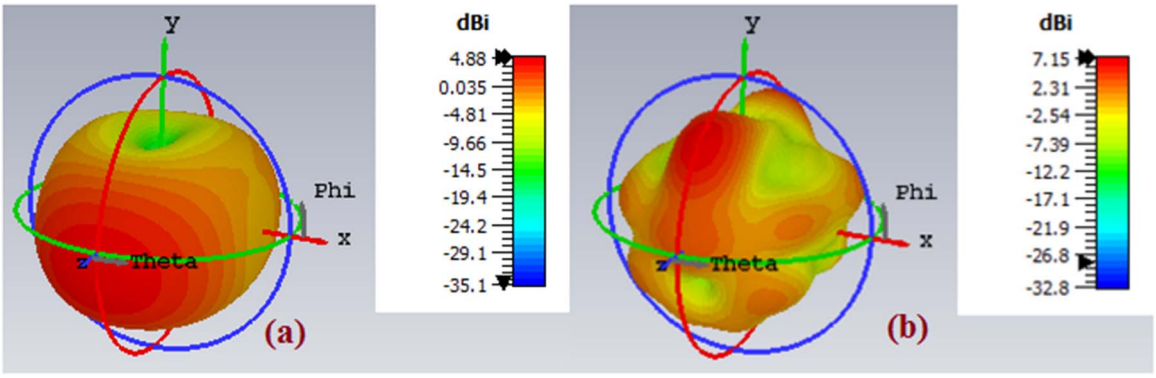



**Figure 14.** Simulated 3D-gain radiation patterns of the proposed antenna-2: (a) 2.45 GHz and (b) 7.56 GHz.

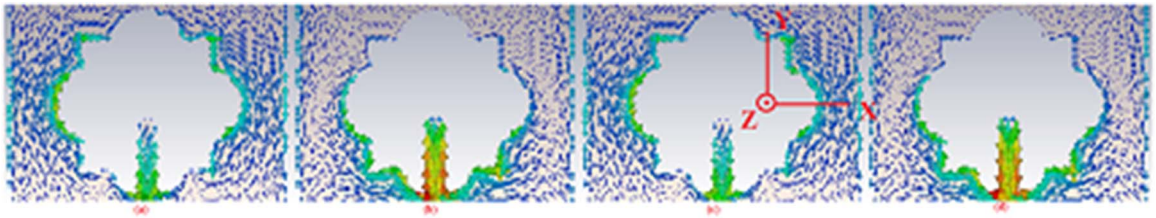



**Figure 15.** Surface current distributions of the proposed antenna-1 at 2.16 GHz: (a) $\omega t=0^{o}$, (b) $\omega t=90^{o}$, (c) $\omega t=180^{o}$, and (d) $\omega t=270^{o}$.

power transmission make it feasible. The receiving antenna, load resistor, rectifier, DC pass filter, and impedance matching network make up the apparatus known as the antenna. A matching network and a high-efficiency rectifier are required to install a full rectenna. The most exciting technologies nowadays are wireless power transfer and RF energy harvesting. The Internet of Things, autonomous wireless sensor networks, and low-power electrical devices can all benefit from this energy. One device that can be used to receive electromagnetic power from ambient RF sources and transform it into DC power is the rectenna (rectifier+antenna). The GSM1800 MHz band is commonly utilized in cellular communication systems and has a 1 W (30 dBm) radiation output. When it comes to wireless power transfer and RF energy harvesting, the receiving antenna is crucial. because environmental sources could provide it with radiofrequency radiation. Wi-Fi routers and cellular base stations provide us with a large amount of low-input RF power in the surroundings. Multiband, multipolarized, omnidirectional, and broad beam efficiency receiving antennas are needed to extract these low RF power-high gain signals. Since transmitting and receiving antennas are not electromagnetically coupled to one another in far-field applications, coupling efficiency is not necessary in this case. The implementation of the rectenna involves merely matching the rectifying circuit's input impedance to the antenna's input impedance. In the construction of the rectifier, the impedance matching network is a crucial secondary function. Microstrip transmission lines are used in the design of the matching circuit. A two-port distributed network, the transmission line is useful for moving electromagnetic energy from one location to another. It must match the antenna's input impedance to the rectifier's input impedance in order to transfer the most power possible from the receiving antenna to therectifier.

## Dual-band antennas for wireless communication

### *Antenna design details*

The proposed slot antennas' basic design geometry is shown in Figure 8. As seen in Figure 8(a), the quatrefoil shape consists of four concentric circles with an equal radius of $r = 12$ mm and one square with a side length of $L = 40$ mm.

However, the symmetrical structure of 24-sided polygon with the side lengths of $L_1 = 10$ mm, $L_2 = 7$ mm, $L_3 = 5$ mm, $L_4 = 7$ mm, $L_5 = 5$ mm, $L_6 = 7$ mm, and the diameter of $D = 50$ mm as shown in Figure 8(b). The schematic and fabrication prototypes of a compact dual-band slot antenna for wireless power transmission and communication are shown in Figure 9 and Figure 10. The antennas are designed on the FR4 substrate with a dielectric constant of 4.3 and a thickness of 1.6 mm. The substrate dimension of antenna-1 is 80 mm × 80 mm ($L_s \times W_s$) and antenna-2 is 85 mm × 80 mm ($L_s \times W_s$). Similarly, the length of the feed line for antenna-1 is 35 mm and for antenna-2 is 39 mm, respectively. The dual-band slot is excited by the 50Ω feed line of width $W_f = 3.1$ mm.

### *Simulation and measurement results*

The CST Microwave Studio full-wave simulator is used to develop and simulate the proposed dual-band slot antennas based on their fundamental geometry. The Agilent Technologies E8363C PNA network analyzer is used for measurement. Figure 11 illustrates how the reflection coefficient $S_{11}$ varies with two antennas' varying FLs. At FL = 35 mm, the proposed antenna-1 resonates the consistent dual band of 2.16 and 6.57 GHz with $S_{11} \geq -25$ dB for both bands.

https://doi.org/10.1017/S1759078726103547 Published online by Cambridge University Press

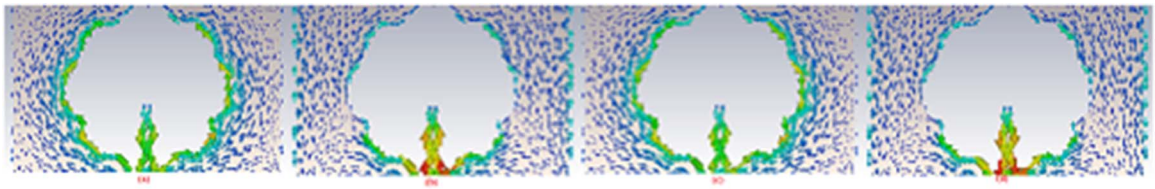


**Figure 16.** Surface current distributions of the proposed antenna-2 at 2.45 GHz: (a) $\omega t=0^{o}$, (b) $\omega t=90^{o}$, (c) $\omega t=180^{o}$, and (d) $\omega t=270^{o}$.

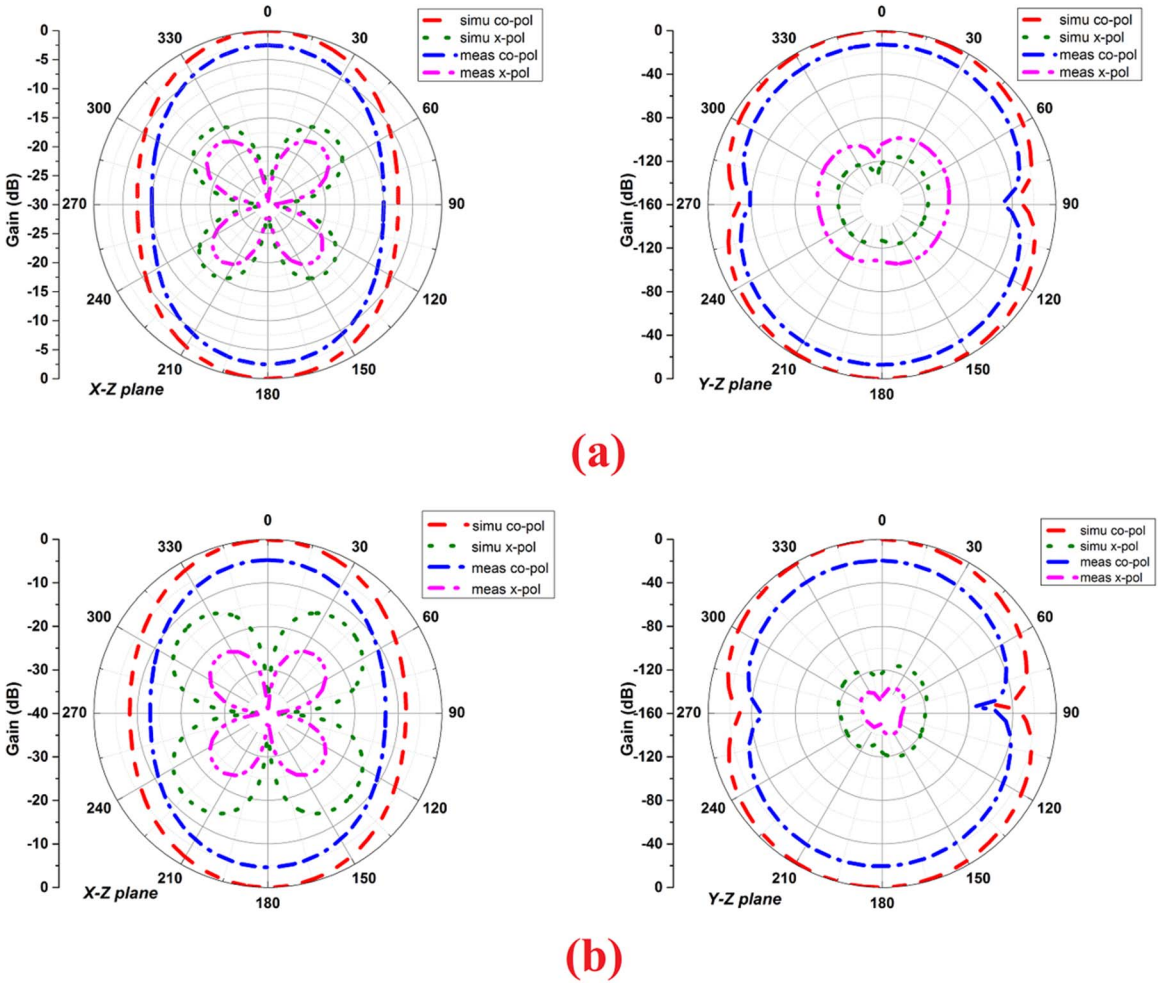



**Figure 17.** Simulated and measured radiation patterns of the proposed antennas: (a) antenna-1 at 2.16 GHz and (b) antenna-2 at 2.45 GHz.

Nevertheless, with FL = 39 mm, the suggested antenna-2 operates on the double-band of 2.45 and 7.56 GHz with $S_{11} \geq -18$ dB on the two bands, respectively. RF power from mobile and lower Wi-Fi bands can be harvested using the first band of two antennas. In a similar way, communication can be facilitated by another band of two antennas. It is significant to note that, due to the symmetrical construction of the suggested slots and an appropriate ground plane, the two antennas' reflection coefficient curves at various FLs display stable dual bands with significant bandwidth and resonance. Figure 12 displays the two suggested antennas' modeled and tested reflection coefficient plots. The simulated findings and measured coefficient of reflection of the two antennas' first band match quite well. However, because of soldering and fabrication tolerances, the second band of the two antennas matches simulation results with little fluctuation. When calculating the antenna received power, the receive antenna gain is a crucial component.

Figure 13 and Figure 14 depict the simulated 3D-gain radiation patterns of the suggested antennas. The square slot of the suggested antenna-1 resonates at the fundamental frequency of 2.3 GHz with a slot length of L = 40 mm (from Figure 8), as determined theoretically using equation (1).

$$f = \frac{c}{2L}\sqrt{\frac{2}{\epsilon_r + 1}} \tag{1}$$

Additionally, for the symmetrical structure and to create the dual-bands, four circular slots with an equal radius of 12 mm are

https://doi.org/10.1017/S1759078726103547 Published online by Cambridge University Press

added to the square slot. Nonetheless, the circular slot's dimension of D = 50 mm (from Figure 8) and resonant frequency of 1.7 GHz were also determined using the following equation (2).

$$f = \frac{1.841c}{2\pi a\sqrt{\epsilon_r}} \quad (2)$$

where $a$ = radius of circular slot (25 mm).

Antenna-1's simulated gain at 2.16 and 6.57 GHz is 3.88 and 4.89 dBi, respectively. Similarly, an antenna-2's simulated gain at 2.45 and 7.56 GHz is 4.88 and 7.15 dBi, respectively. On the other hand, the network analyzer with the equation fulfilled for the far-field distance between the transmitting and receiving antennas is used to measure the gain. The measured gains were 3.27 and 4.36 dBi at antenna-1's dual-band center frequencies and 4.15 and 6.83 dBi at antenna-2's dual-band center frequency, respectively. Figure 15 and Figure 16 show the surface current patterns of the suggested antennas at various time periods. The two antennas' current vectors have a positive y-direction at $\omega t=0^o$ and a negative y-direction at $\omega t=90^o$ . Similarly, for the two antennas, the current distribution is seen in the negative y-direction at time instance $\omega t=90^o$ and in the positive y-direction at time instance $\omega t=270^o$ . At the dual-band center frequency, antenna-1's simulated radiation efficiencies are 85.39% and 71.32%. In the same way, antenna-2's simulated radiation efficiencies at the dual-band center frequency are 99.15% and 95.60%, respectively. Figure 17 displays the computed and measured radiation characteristics of the suggested double-band slotted antennas operating at 2.16 and 2.45 GHz energy harvesting frequencies. For innovative applications of dynamic switching of dual frequencies without the need for an external DC control signal, a self-powered frequency-tunable antenna and differential frequency reconfigurable rectifier coupled antenna can be employed successfully. In the future, circularly polarized rectifying metamaterial antennas and polarization conversion rectifying metasurfaces for Radio Frequency Energy Harvesting (RFEH) and Wireless Power Transmission (WPT) applications could be investigated. For energy harvesting, it is ideal to receive a significant quantity of electromagnetic radiation from all polarizations. Future 5G rectennas that exploit millimeter-wave energy harvesting at low input power levels are the antenna engineers' primary emphasis. In millimeter-wave energy harvesting, the choice of substrates and rectifying diode is essential. Furthermore, the coupling of wireless communication with power electronics is an amazing field of study for applications involving simultaneous wireless data transfer and power transmission.

## Conclusion

This work presents double-band slot antennas with configurable FL. Theoretical analysis of the antenna's performance was done using mathematical formulas, and the FL was changed without changing the antenna's dimensions. The proposed slots' symmetrical structure and the appropriate ground plane are selected to resonate the necessary dual bands. For the purpose of designing rectifier circuits, these antennas offer adequate gain, radiation efficiency, energy density, and received power values. The suggested antennas are beneficial for simultaneous wireless information and power transmission applications, according to the final findings. For triple-band GPS/WLAN/ISM band operations, a small planar slotted monopole antenna is presented in this work. Using simulation findings, the regulation of individual frequencies with circular and inverted L-slots is described. Analysis was also done on the radiation patterns and the dispersion of surface currents. The findings of the measurements and the simulations correspond quite well. The proposed antenna is formidably suitable for multiband independent frequency tuning applications.

**Competing interests.** The authors declare no competing interests.

## References


1. **Sung Y** (2015) Simple inverted-F antenna based on independent control of resonant frequency for LTE/wireless wide area network applications. *IET Microwaves Antennas and Propagation* 553–560.
2. **Cao Y, Cheung W and Yuk T** (2015) A multiband slot antenna for GPS/WiMAX/WLAN systems. *IEEE Transactions on Antennas and Propagation* 952–958.
3. **Qu L, Zhang R and Kim H** (2015) Compact dual-band antenna using inverted-L loop and inner rectangular loop for WLAN applications. *Electronics Letters* 1843–1844.
4. **Wu MT and Chuang L** (2015) Multi broadband slotted bow-tie monopole antenna. In *IEEE Antennas and Wireless Propagation Letters*, pp. 887–890.
5. **Qu L, Zhang R, Lee H and Kim H** (2016) Compact triple-band ground radiation antenna using two inner rectangular loops enclosed by two outer loops. *Electronics Letters* 790–792.
6. **Qian F, Chen F, Xiang R and Chu Q** (2019) Resonator loaded multi-band microstrip slot antennas with bidirectional radiation patterns. *IEEE Transactions on Antennas and Propagation* 6661–6666.
7. **Bakariya P, Santanu D, Manas S and Mandal MK** (2015) Proximity-coupled microstrip antenna for bluetooth, WiMAX, and WLAN applications. In *IEEE Antennas and Wireless Propagation Letters*, pp. 755–758.
8. **Qian J, Chen F and Chu X** (2018) A novel tri-band patch antenna with broadside radiation and its application to filtering antenna. *IEEE Transactions on Antennas and Propagation* 5580–5585.
9. **Sarkar D, Saurava K and Srivatsava K** (2014) Multi-band microstrip-fed slot antenna loaded with split ring resonator. *Electronic Letters* 1498–1500.
10. **Varma R, Ghosh J and Bhattacharya R** (2017) A compact dual frequency double U-slot rectangular microstrip patch antenna for WiFi/WiMAX. *Microwave and Optical Technology Letters* 2174–2179.
11. **Li K, You C, Yu F, Cheng J, Yang W and Deng H** (2018) A high frequency ratio quadri-band frequency independently tunable antenna with spurious-mode suppression. *Microwave and Optical Technology Letters* 1445–1452.
12. **Abdelheq B, Lin XQ, Jia Wei Y and Mei P** (2017) Yuan Jiang, and Yi Qiang Yu: A Highly Integrated Independently Tunable Triple-Band Patch Antenna. In *IEEE Antennas and Wireless Propagation Letters*, pp. 2216–2219.
13. **Lei G, Mingjian L, Wang J and Hui G** (2017) Unidirectional Dual-Band Stacked Patch Antenna With Independent Frequency Reconfiguration. *IEEE Antennas and Wireless Propagation Letters* **16**, 113–116.
14. **Islam N, kumar M, Sen G and Das S** (2018) Design of a compact quad-band antenna with independent frequency tuning. *Electronic Letters* 920–922.
15. **Sandhya C and Akhtar MJ** (2020) An efficient dual-band rectenna using symmetrical rectifying circuit and slotted monopole antenna array. *International Journal of RF and Microwave Computer Aided Engineering* 1–15.
16. **Shi Y, Fan Y, Yang L, Pang J, Jing J and Wang M** (2018) Efficient RF energy harvest with a novel broadband vivaldi rectenna. *Microwave and Optical Technology Letters* 2420–2425.
17. **Hussain R, Khan MU and Sharawi MS** (2021) Dual-band slot-based MIMO antenna design with independent tuning. In *IEEE International Symposium on Antennas and Propagation and North American Radio Science Meeting*, pp. 1757–1758.
18. **Dang QH, Chen SJ, Ranasinghe DC and Fumeaux C** (2023) Dual-band reconfigurable flexible antenna With independent frequency tunability. In *IEEE Antennas and Wireless Propagation Letters*, pp. 531–535.


https://doi.org/10.1017/S1759078726103547 Published online by Cambridge University Press

19. **Wang S, Li HC, Yin Li ZCG, Zhang G, Yang L and García RG** (2024) A wideband end-fire stepped slot antenna with gain enhancement and filtering capability. *IET Microwaves Antennas and Propagation* 422–429.
20. **Rakluea P, Wongsin N, jatuphat CM, Aroonmitr P, Jangjing T, Rakluea C, Chanwattanapong W and Chudpooti N** (2023) Flexible thin film-based triple port UWB MIMO antenna with modified ground plane for UWB,WLAN, WiMAX, WPAN and 5G Applications. *IEEE Access* 107031–107048.
21. **Mohamed A-R, Ahmed HE and Ramesh KP** (2017) Design of a dual-band microstrip antenna with enhanced gain for energy harvesting applications. In *IEEE Antennas and Wireless Propagation Letters*, pp. 1622–1626.
22. **Palazzi V, Hester J, Jo Bito FA and C** (2018) Kalialakis: A novel ultra-lightweight multiband rectenna on paper for RF energy harvesting in the next generation LTE bands. *IEEE Transactions on Microwave Theory and Techniques* 366–379.
23. **Khemar A, Abdellah Kacha HT and Abib G** (2018) Design and experiments of a dual-band rectenna for ambient RF energy harvesting in urban environments. *IET Microwaves Antennas & Propagation* 49–55.
24. **Shen S, Chiu C-Y and Murch RD** (2017) A dual-port triple-band L-probe microstrip patch rectenna for ambient RF energy harvesting. In *IEEE Antennas and Wireless Propagation Letters*, pp. 3071–3074.
25. **Kamoda H, Kitazawa S, Kukutsu N and Kobayashi K** (2015) Loop antenna over artificial magnetic conductor surface and its application to dual-band RF energy harvesting. *IEEE Transactions on Antennas and Propagation* 4408–4417.
26. **Niotaki K, Kim S, Jeong S and Collado A** (2013) A compact dual-band rectenna using slot-loaded dual-band folded dipole antenna. In *IEEE Antennas and Wireless Propagation Letters*, pp. 1634–1637.
27. **Kuhn V, Lahuec C, Seguin F and Person C** (2015) A multi-band stacked RF energy harvester with RF-to-DC efficiency up to 84%. *IEEE Transactions on Microwave Theory and Techniques* 1768–1777.
28. **Liu YW, Lu YJ and Hsu P** (2014) Harmonic suppressed slot loop antenna fed by coplanar waveguide. In *IEEE Antennas and Wireless Propagation Letters*, pp. 1292–1295.
29. **Wang M, Fan Y, Yang L, Li Y, Feng J and Shi Y** (2019) Compact dual-band rectenna for RF energy harvest based on a tree-like antenna. *IET Microwaves Antennas and Propagation* 1350–1357.
30. **Li W, Wang Y, You B, Shi Z and Liu QH** (2018) Compact ring slot antenna with harmonic suppression. In *IEEE Antennas and Wireless Propagation Letters*, pp. 2459–2463.
31. **Tejpal VT, Dinesh Yadav SR and Bhatnagar D** (2018) Wideband circularly polarised antenna with an asymmetric meandered-shaped monopole and defected structure for wireless communication. *IET Microwaves Antennas & Propagation* 2305–2317.
32. **Tejpal VT, Dinesh Yadav SR and Bhatnagar D** (2016) Dual-Band Rectenna for Ambient RF Energy Harvesting at GSM 900 MHz and 1800 MHz. In *IEEE International Conference on Sustainable Energy Technologies*, pp. 306–310.



**Geriki Polaiah** received the M.Tech. degree in electronics and communication engineering from Jawaharlal Nehru Technological University Anantapur, India, in 2010 and a Ph.D. degree in electronics and communication engineering from National Institute of Technology Karnataka, Surathkal, Mangalore, India. His current research interests include computational electromagnetics, microwave antennas, RF integrated circuits for wireless power transmission, and energy harvesting applications.

https://doi.org/10.1017/S1759078726103547 Published online by Cambridge University Press